Capillary rise in foams under microgravity

H. Caps[†], S.J. Cox[‡], H. Decauwer[⋆]
D. Weaire[‡] and N. Vandewalle[†]

[†] *GRASP, Department of Physics B5, Université de Liège, 4000 Liège, Belgium*

[‡] *Department of Physics, Trinity College, Dublin 2, Ireland*

[⋆] *ATI, Department of Astrophysics B5a, Université de Liège, 4000 Liège, Belgium*

Abstract

The motion of liquid into a foam under low gravity conditions is studied both experimentally and theoretically. The foam is confined to two dimensions in a Hele-Shaw cell and the liquid fraction measured by image analysis. The foam imbibition is shown to be a diffusive process. Two models are analysed, corresponding to the limits of rigid and mobile interfaces in the Plateau borders. Liquid fraction profiles are compared to experimental ones.

Key words: Aerosols and foams, Emulsions and foams, Testing in microgravity environments
PACS: 82.70.Rr, 83.80.Iz, 81.70.Ha

1 Introduction

The fluid motion through the network of Plateau borders that make up a foam is a complex problem involving various physical processes such as capillarity, gravity and viscosity [1]. The study of such phenomena is of great interest since they play an important role during the life of a foam, from the foam production (bubbling/nucleation) to the foam decay (bubble popping/coalescence).

On Earth, gravitational forces cause most of the liquid to drain out of the foam. This drainage destabilizes the foam and changes its rheological properties. Thus, in both fundamental research and industrial applications drainage is important. In research it is desirable to avoid such an effect, and for this the microgravity environment appears as a useful solution.

In this paper, we present the results of microgravity experiments on aqueous foams [2], in which liquid invades the foam from below [3]. These were per-

formed during a parabolic flight campaign organized by the European Space Agency (ESA). About 30 parabolas each allowing 20 s of microgravity were dedicated to this experiment. A theoretical description of the problem based upon drainage theory is given in two limiting cases, showing how the surface viscosity of the interfaces in the foam plays a key role. Comparison between experiments and theory confirms the validity of drainage theory.

2 Experiments

The experimental setup consisted of a vertical Hele-Shaw (HS) cell filled with a few millilitres of soap-water mixture [2]. The commercial soap was mainly composed of dodecylsulfate (surface tension $\sigma = 3.0 \times 10^{-2}$ N/m, viscosity $\eta = 1 \times 10^{-3}$ N s/m^2). The HS cell was a closed rectangular ($20 \times 20 \times 0.2$ cm^3) vessel made of Plexiglas. Its thickness was such that only one layer of bubbles was allowed, i.e. the foam was two-dimensional. Microgravity prevailed during 20 s of each of the 30 parabolas described by the aircraft. Before each parabola, the HS cell was shaken in order to create the foam. The bubbles had a typical diameter $\ell = 5$ mm. During the flight, a CCD camera recorded the foam evolution. Liquid fractions, interpreted as the thickness of the Plateau borders (PBs) pressed against the wall of the cell, were later measured by image analysis. On each image of the movie, a threshold is applied in order to emphasize the PBs. Then, at a given height in the cell, the liquid fraction is given by the mean width of the PBs compared to the width of the cell.

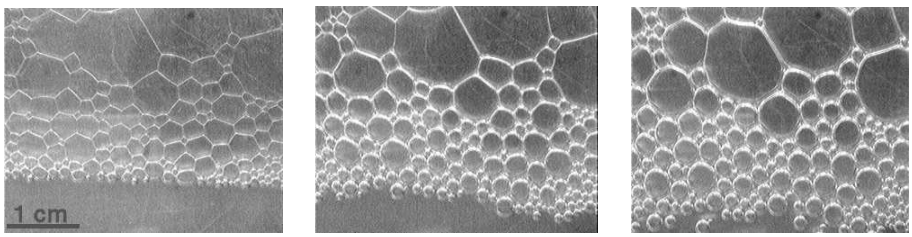

Fig. 1. Illustrations of part of a 2D foam in a Hele-Shaw cell during a single parabola: (left) hypergravity (2g) phase, (centre) 1 s after microgravity is established, (right) after 15 s of microgravity.

In Figure 1 a part of the foam is presented during both hyper- and microgravity phases. The hypergravity phase (left picture) led to a general drying of the foam. Except near the foam/liquid interface where the foam was composed of small "wet" circular bubbles, polygonal bubbles were observed. Some motion of the small bubbles was observed at the bottom due to the aircraft vibrations.

When microgravity was attained, the situation changed drastically: the liquid invaded the foam from below so that the average thickness of all PBs increased, as seen in Figure 1. The bubbles became more rounded and slipped past each

other. Aircraft vibrations caused them to move freely in the fluid. Moreover, the foam *inflated* and invaded the liquid phase. When the microgravity phase ended, an acceleration of about $2g$ led to a fast and global drainage of the foam and it returned to the initially dry situation quite rapidly.

The capillary rise of the liquid into the foam is clearly revealed by the profiles of liquid fraction, Φ_l. A typical temporal evolution of such a profile is presented in Figure 2. At first, the bottom of the foam was wet ($\Phi_l \approx 35$ %) while the top was dry ($\Phi_l \approx 5$ %). As time increased, the amount of liquid in the foam increased. This caused the foam inflation and rigidity loss [2]. It should be noted that the small growth of Φ_l at ≈ 1 cm height for large times comes from the downwards motion of small bubbles that create empty regions.

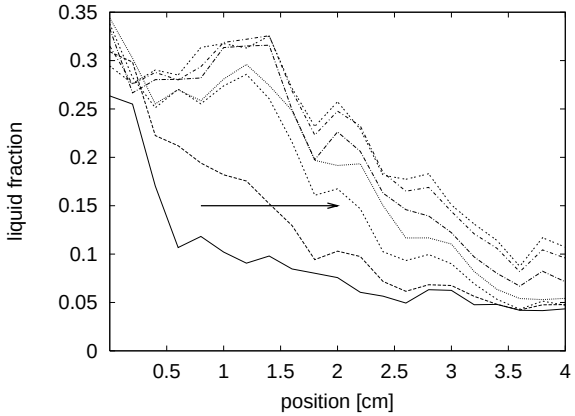

Fig. 2. Typical experimental profiles of the liquid fraction evolution. The amount of liquid in the foam increased over time. From left to right, profiles correspond to times : 4 s, 8.8 s, 9.6 s, 10 s, 10.8 s, 11.6 s, 12 s

The imbibition is characterized by a liquid front propagating into the foam. No fingering was observed. We measure the position of the front at a given time by finding the highest point at which the liquid fraction rises rapidly above its equilibrium value. (In Figure 2, the earliest (lowest) profile of liquid fraction at time $t = 4$ s shows the front at a position 2.5 cm above the base of the foam.) As a function of time, this wetting front is seen to rise in the liquid according to a square-root law (see Figure 3):

$$h = \sqrt{D\,(t - t_0)}\,, \tag{1}$$

where, without loss of generality, we choose the time $t_0 = 0$ as the beginning of the microgravity stage. D is the diffusivity, measured as $D = 1.19 \pm 0.07$ $\mathrm{cm^2\,s^{-1}}$, which characterizes the capillary rise. The velocity of this front depends on geometric properties of the foam as well as on the surfactant chemistry, as shown below.

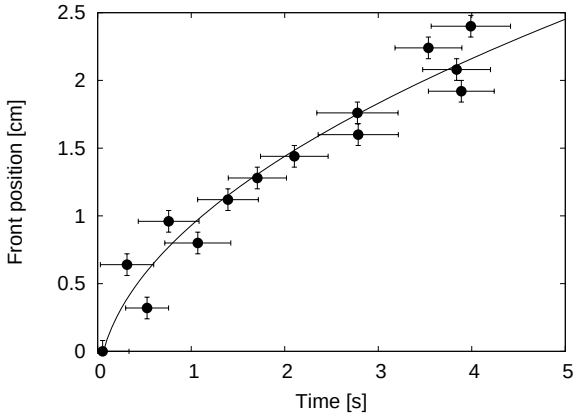

Fig. 3. The position of the wetting front that moved through the foam after the microgravity phase commenced. The measurement is taken at a value of 5% liquid fraction, since this is the driest value at the start of the microgravity phase. A square-root law in which the position of the front increases with time was observed [2].

3 Comparison with theory

The theoretical approach to analyzing such experiments [4] is based upon the use of partial differential *drainage* equations. These, generally nonlinear, diffusion equations [1,5] describe the evolution of the liquid profile in the network of PBs. That is, they neglect any flow through the soap films, since these make only a small contribution to the volume of liquid in the foam. The effects of surface rheology on the drainage process are poorly understood, leading us to consider two limiting cases which provide bounds on the rapidity with which liquid moves into the foam [6]. We can solve these equations to give the profiles of liquid fraction and the position of the wetting front that invades a dry foam, without recourse to free fitting parameters.

The first equation is based upon Poiseuille flow through the PBs, while the second assumes a plug flow in the PBs, with viscous dissipation occurring in the vertices where they meet. The former appears to be appropriate for foams made from surfactants with high surface viscosity ("rigid interfaces"), such as the commercial detergent "Fairy Liquid", and emulsions, while the latter describes surfactants with low surface viscosity ("mobile interfaces") such as pure SDS [7]. These are recognised as two limiting cases, with real foams often lying close to one or other of the limits. However, the details of the interpolation between these limits remains to be fully understood.

The diffusion equations express the variation of PB area A with position x and time t. For our purposes it is sufficient to take parameter values for a monodisperse, hexagonal bubble structure: the average length of a PB is taken as the relevant length-scale. Rather than a global average, we choose a value

of the length-scale appropriate to the small bubbles near the bottom of the foam, $L = 1$ mm. Comparison between the experimental and numerical results suggests that the front velocity is governed by these small bubbles rather than the mean bubble size.

The liquid fraction is then given by the total length of PBs associated with each bubble, divided by the bubble volume. For each bubble there are 6 PBs of length H that span the gap between the plates and are shared by three bubbles, and 12 PBs of length L that lie along the plates and are each shared by two bubbles. Thus

$$\Phi_l = \frac{2A(6L + 2H)}{3\sqrt{3}L^2H} \approx 1.92\frac{A}{L^2}.$$

where H is the thickness of the HS cell.

A slight change to the familiar drainage equations is entailed by the change in geometry – the experiments were two-dimensional, so the liquid-transporting PBs are pressed against the walls of the Hele-Shaw cell, i.e. we assume that liquid transport through the PBs of length H, spanning the gap between the plates, is negligible.

The time-scale is given by

$$T = \frac{\eta L}{\delta \sigma K}$$

where the geometrical constant is $\delta = (\frac{1}{2}(4 - \pi))^{1/2} \approx 0.655$. The parameter K measures the permeability of the foam; its value depends upon the nature of the flow, and thus on the choice of model. In the rigid-interface case it is found from the velocity profile of Poiseuille flow in each PB, and it can be shown that K_r varies little between PBs in the bulk and on the surface of a foam. We use the value $K_r = 9.9 \times 10^{-3}$. (This includes a factor of one-half, due to averaging the possible orientations of a PB in two dimensions.) The permeability in the mobile-interface case is governed by the shearing flow in the vertices. It has been obtained empirically [5,8] for bulk vertices with a value of $K_m = 2.3 \times 10^{-3}$. In the absence of experiments on the dissipation in surface vertices, we must here assume that it also does not vary greatly and use this value. The relevant time-scales are then $T_r = 5.14 \times 10^{-3}$ s and $T_m = 2.21 \times 10^{-2}$ s.

In each case, we reduce the equations to a dimensionless form, using $\alpha = A/L^2$, $\xi = x/L$ and $\tau = t/T$, to give

$$\frac{\partial \alpha}{\partial \tau} = \frac{\partial}{\partial \xi}\left(\frac{\sqrt{\alpha}}{2}\frac{\partial \alpha}{\partial \xi}\right) \qquad \text{RIGID INTERFACES} \tag{2}$$

and

$$\frac{\partial \alpha}{\partial \tau} = \frac{\partial}{\partial \xi}\left(\frac{1}{2}\frac{\partial \alpha}{\partial \xi}\right) \qquad \begin{matrix}\text{MOBILE}\\ \text{INTERFACES}\end{matrix} \tag{3}$$

which is the diffusion equation.

We set $\alpha(\xi = 0, \tau) = \alpha_0$, where the parameter α_0 corresponds to the critical liquid fraction $\Phi_l \approx 35\%$ at which the foam becomes a bubbly liquid. The appropriate solutions of (2) and (3) are shown in Figure 4. Note that in the second case, an exact solution exists in the form of an error function [6], while we solve the former numerically.

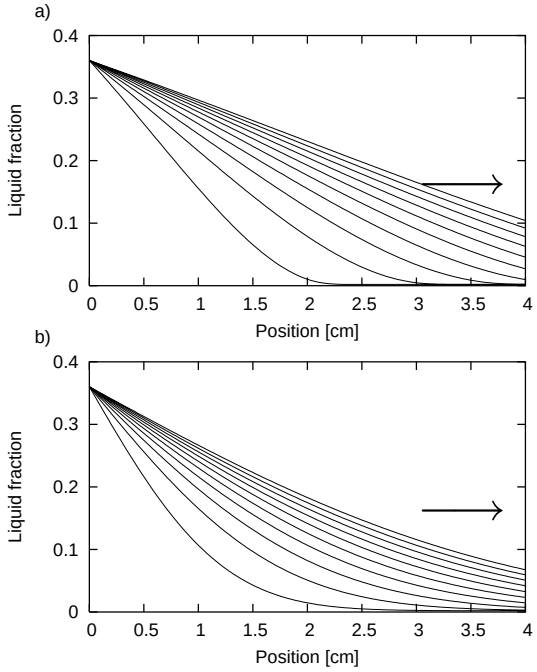

Fig. 4. Profiles of liquid fraction are shown at 2 second intervals in each of both cases: (a) Rigid interfaces, (b) Mobile interfaces. Although the foam extends to a height of 20 cm, only the 4 cm of the foam closest to the liquid pool are shown,

In both cases, analysis of the drainage equations in (2) and (3) shows that the amount of liquid in the foam increases with the square-root of time. The position of the wetting front also increases with the square-root of time, as shown in Figure 5. We measure a diffusion coefficient in each case, in the form $D = L^2/T$, the difference being due to the variation in the permeability constant K. For rigid interfaces we have $D = 1.94$ cm^2 s^{-1} while for mobile interfaces it is $D = 0.452$ cm^2 s^{-1} [9]. As expected, the value measured in the experiments lies between these two extremes.

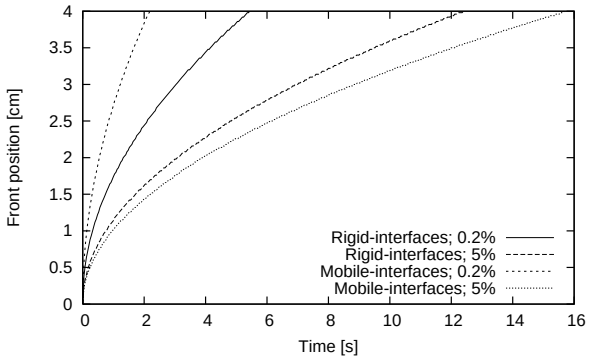

Fig. 5. The position of the wetting front that moves through the foam after the microgravity phase commences increases with the square-root of time. The value of liquid fraction at which the position of the front is calculated is arbitrary: we take it to be the most distant point from the origin that has liquid fraction greater than either 0.2% or 5%; the latter case is compared with experiment below. In the mobile-interface case the foam is slightly wetted everywhere very rapidly (compare the profiles at 0.2% liquid fraction), but the bulk of the liquid enters the foam more quickly in the rigid-interface case (compare the profiles at 5% liquid fraction). As the value of liquid fraction at which the front is calculated is increased, the velocity of the front decreases.

4 Conclusions

The experimental results have shown that foam imbibition in low-gravity environment is a diffusive process. For the sample used, the liquid front propagation from bottom to top is characterized by a diffusivity $D = 1.19 \pm 0.07$ $\mathrm{cm}^2\,\mathrm{s}^{-1}$. Theoretical predictions have shown that this behavior lies in-between the expected limits of rigid and mobile interfaces with $D = 1.94$ cm^2 s^{-1} and $D = 0.452$ cm^2 s^{-1} respectively.

Both liquid fraction profiles and front propagation dynamics are well reproduced by the drainage theory, as emphasized by Figure 6 where theoretical predictions of the front position as a function of time are compared with experimental data.

It should be noted that the experimental value of D depends on the surfactant molecules as well as on the bubble size and liquid fraction. Both surfactant and foam properties play a role in the selection of the flow regime. In the future, experiments with well defined surfactants would surely help in emphasizing the key parameters.

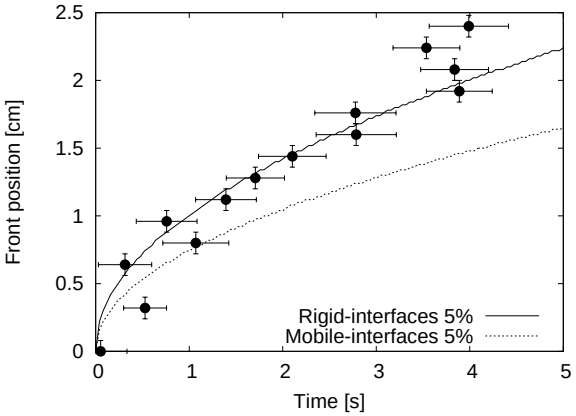

Fig. 6. The position of the wetting front that moves through the foam after the microgravity phase commences. Theoretical predictions in both cases of rigid and mobile interfaces are also shown, illustrating the excellent agreement between theory and experiment.

Acknowledgements

HC and HD benefited from a FRIA (Brussels, Belgium) fellowship. This work was also supported by ESA through the project AO-99-108.

References

[1] D. Weaire and S. Hutzler. 1999. *The Physics of Foams.* Clarendon Press, Oxford.

[2] H. Caps, H. Decauwer, M.-L. Chevalier, G. Soyez, M. Ausloos and N. Vandewalle. 2003. Foam imbibition in microgravity. *Euro. Phys. J. B* **33**:115–119.

[3] D.A. Noever and R.J. Cronise. 1994. Weightless bubble lattices: A case of froth wicking *Phys. Fluids* **6**:2493–2500.

[4] S.A. Koehler, H.A. Stone, M.P. Brenner and J. Eggers. 1998. Dynamics of foam drainage. *Phys. Rev. E* **58**:2097–2106.

[5] S.A. Koehler, S. Hilgenfeldt and H.A. Stone. 2000. A generalized view of foam drainage: Experiment and theory. *Langmuir* **16**:6327–6341.

[6] S.J. Cox and G. Verbist. 2003. Liquid flow in foams under microgravity. *Microgravity Science and Technology* **XIV/4**:45–52.

[7] M. Durand, G. Martinoty and D. Langevin. 1999. Liquid flow through aqueous foams: From the plateau border-dominated regime to the node-dominated regime. *Phys. Rev. E* **60**:R6307–R6308.

[8] M.U. Vera and D.J. Durian. 2002. Enhanced drainage and coarsening in aqueous foams. *Phys. Rev. Lett.* **88**:088304.

[9] S.J. Cox, D. Weaire and G. Verbist. 2004. Comment on "Foam imbibition in microgravity. An experimental study". *Euro. Phys. J. B.* **40**:119–121.